tric Liquid Crystal," *Appl. Phys. Lett.*, Vol. 54, No. 15, 1989, pp. 1394–1396.
11. B. E. A. Saleh and M. C. Teich, *Fundamentals of Photonics*, John Wiley & Sons, Inc., New York, 1991.

Received 5-27-96

Microwave and Optical Technology Letters, 13/6, 351–354

CCC 0895-2477/96

A GENERALIZED METHOD FOR TWO DIMENSIONAL SCATTERING PROBLEMS UNDER TE INCIDENCE WITH THE USE OF SPECTRAL TECHNIQUES

J. M. López, V. E. Boria, M. Baquero, and M. Ferrando
Departamento de Comunicaciones
Universidad Politecnica
Camino DeVera S/N
46071 Valencia, Spain

KEY TERMS

Scatterer transference matrix, spectral techniques, method of moments

ABSTRACT

A new method for characterizing electrically large scatterers and solving the scattering of multiple objects in two dimensions for TE polarization of the incident field is presented. Large objects are divided into smaller ones. The method of moments and spectral techniques are used to compute a transference matrix for each single subscatterer, which relates the incident and scattered fields. Then, with the use of an iterative method for solving the interaction between all of them, the response for the whole system is obtained. This procedure is more efficient than the method of moments when applied to the scatterer considered as a single element. © 1996 John Wiley & Sons, Inc.

1. INTRODUCTION

Up to now, electrically large objects have been studied with the use of costly high-frequency techniques like physical optics and GTD, because other numerical techniques like the method of moments are inefficient for such problems. An alternative procedure to solve such problems is presented in this article. First of all, the scatterers are divided into smaller subobjects, which are easily studied by means of the well-known method of moments [1], which is quite accurate and efficient for electrically small scatterers. Each subobject is represented by a transference matrix that relates the spectra of the incident and scattered fields, making the problem independent of the geometry of each individual subobject. Finally, an iterative method, described in [2], is used here in order to find the field scattered by the whole object when an arbitrary incidence with TE polarization is present.

A two-dimensional TE field in isotropic media has no z component of **E** and only has a z component of **H**. Therefore, it is convenient to use the magnetic field for TE cases because the solutions of the electromagnetic problems are reduced to the ones of scalar problems.

2. TRANSFERENCE MATRIX OF A SINGLE SCATTERER

Metallic objects with no z dependence are treated. Such objects can be enclosed by an imaginary cylinder, and the incident field to this cylinder and the scattered field by the object can be expressed in terms of a series of cylindrical modes or spectral components:

$$H_z^i = \sum_{p=-N_I}^{N_I} i_p J_p(k\rho) e^{jp\phi}, \tag{1}$$

$$H_z^s = \sum_{q=-N_D}^{N_D} c_q H_q^{(2)}(k\rho) e^{jq\phi}, \tag{2}$$

where ρ and ϕ are defined according to an internal point of this cylinder, as shown in Figure 1.

The i_p and c_q coefficients form two column vectors, $\underline{I}$ and $\underline{C}$, namely, the spectra of the incident and scattered fields, respectively. The purpose of our method is to find a matrix that which relates these spectra by means of a single matrix product,

$$\underline{I} = \underline{D} * \underline{C}, \tag{3}$$

where the d_{qp} element of $\underline{D}$ means the weight of the qth spectral scattered component due to the pth spectral incident component.

The process to compute this matrix is completed by the following four steps:

1. Suppose the incident field is only one of the cylindrical modes $J_p(k\rho)e^{jp\phi}$.
2. Find the surface current density **J** excited on the object by such an incident field.
3. Express the scattered field produced by this current distribution as a series of emergent cylindrical modes. The coefficients of that series will be the pth column of the matrix.
4. Repeat Steps 1–3, running p from $-N_I$ to N_I.

In order to find the surface current density **J**, the method of moments [1] is used. This numerical technique consists of writing the magnetic field integral equation (MFIE) particu-

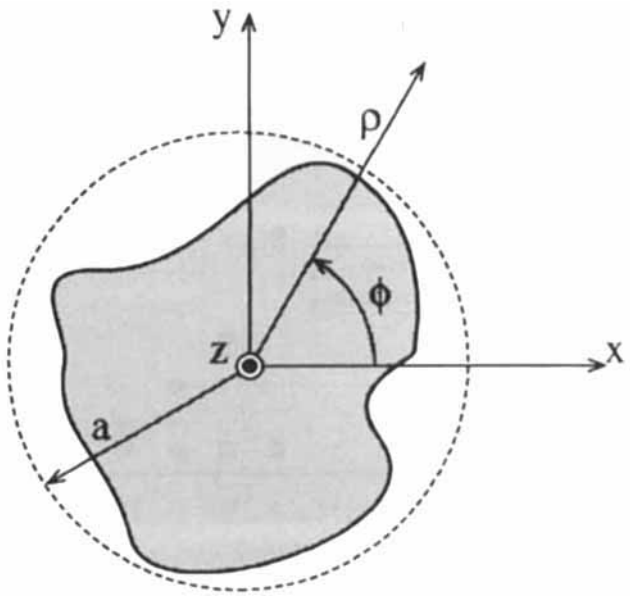

Figure 1 Coordinate system. Arbitrary-shaped object enclosed by a cylinder

larized on the conductor surface. The MFIE relates the tangential components of the incident and scattered fields, H_z^i and H_z^s. It can be expressed through the equation

$$\mathbf{J} = \hat{n} \times \mathbf{H}^i + \hat{n} \times \mathbf{H}^s, \qquad \text{with } \mathbf{H}^s = f(\mathbf{J}). \tag{4}$$

The method of moments reduces this integral equation to a set of algebraic equations solved like a matrix system.

The total magnetic field at any point is $H_z = H_z^i + H_z^s$, H_z^s being the magnetic field produced by $\mathbf{J}$ on the object surface. They are related in the TE case by

$$H_z^s = \hat{z} \cdot \nabla \times \int_C JG\, d\mathbf{l}', \tag{5}$$

where $d\mathbf{l}'$ designates the reference direction of $\mathbf{J}$, and G is the two-dimensional Green's function given by

$$G(\boldsymbol{\rho}, \boldsymbol{\rho}') = \frac{1}{4j} H_0^{(2)}(k|\boldsymbol{\rho} - \boldsymbol{\rho}'|). \tag{6}$$

A section of the object surface is shown in Figure 2. The field H_z is finite external to C, zero internal to C, and the discontinuity equals the current density.

If we take into account the problems that such a discontinuity arises and use the formulation of the method of moments, it is possible to express

$$J = -\left[H_z^i + \hat{z} \cdot \nabla \times \int_C JG\, d\mathbf{l}' \right]_{C_+}, \tag{7}$$

which is the equation for the unknown J. C_+ denotes an evaluation of the magnetic field just external to C. Moreover, if the scatterer is a conducting sheet of infinitesimal thickness, it should be treated as the limit of one of finite thickness. If the point-matching approximation of the method of moments is used, the matrix system to solve is expressed by

$$\underline{I} * \underline{\alpha} = \underline{g}, \tag{8}$$

where

$$g_m = -H_z^i(x_m, y_m), \tag{9}$$

$$I_{mn} = \delta_{mn} + H_z^s(m, n), \tag{10}$$

and α_n are the coefficients employed to develop the unknown J in terms of a series $J = \sum \alpha_n f_n$. f_n are the basis functions of the method, (x_n, y_n) are the coordinates of the central point at each segment ΔC_n (current units) of the basic contour, δ_{mn} is the Kronecker delta, and $H_z^s(m, n)$ denotes H_z^s at (x_m, y_m) on C_+ due to a unit current density on ΔC_n at (x_n, y_n). A typical current unit is depicted in Figure 3.

The final expressions of the I_{mn} elements of the $\underline{I}$ matrix, according to [1], are

$$I_{nn} \approx \tfrac{1}{2}, \qquad m = n, \tag{11}$$

$$I_{mn} \approx \frac{j}{4} k\, \Delta C_n (\mathbf{n} \cdot \mathbf{R}) H_1^{(2)}(k|\boldsymbol{\rho}_m - \boldsymbol{\rho}_n|), \qquad m \neq n, \tag{12}$$

where $\mathbf{n}$ is the unit normal to the element of current and

$$\mathbf{R} = \frac{\boldsymbol{\rho}_m - \boldsymbol{\rho}_n}{|\boldsymbol{\rho}_m - \boldsymbol{\rho}_n|}. \tag{13}$$

The final solution for J is well known and is given by $J = \underline{f} * \underline{I}^{-1} * \underline{g}$, where $\underline{f}$ denotes a vector of basis functions f_n.

Once the surface current density is found, the magnetic field due to the nth element of current (see Figure 4) created by the contour segmentation can be obtained with the use of

$$H_z^s(\boldsymbol{\rho}) = \frac{j}{4} k I_n (\mathbf{n} \cdot \mathbf{R}) H_1^{(2)}(k|\boldsymbol{\rho} - \boldsymbol{\rho}_n|), \tag{14}$$

where $I_n = J(n)\, \Delta C_n$ is the nth element of current and $\mathbf{R}$ is expressed as

$$\mathbf{R} = \frac{\boldsymbol{\rho} - \boldsymbol{\rho}_n}{|\boldsymbol{\rho} - \boldsymbol{\rho}_n|}. \tag{15}$$

If there are N elements of current, the total field is the summation of all the contributions due to each one:

$$H_{z\,\mathrm{TOTAL}}^s(\boldsymbol{\rho}) = \sum_{n=1}^{N} \frac{j}{4} k I_n (\mathbf{n} \cdot \mathbf{R}) H_1^{(2)}(k|\boldsymbol{\rho} - \boldsymbol{\rho}_n|). \tag{16}$$

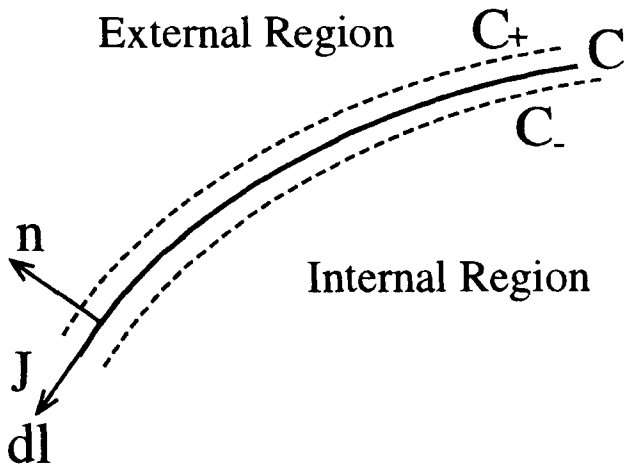

Figure 2 Section of the object surface

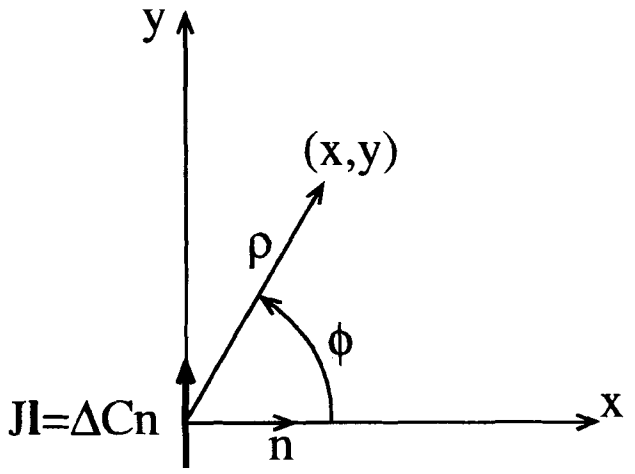

Figure 3 Element of current $J\mathbf{l}$ and local coordinates

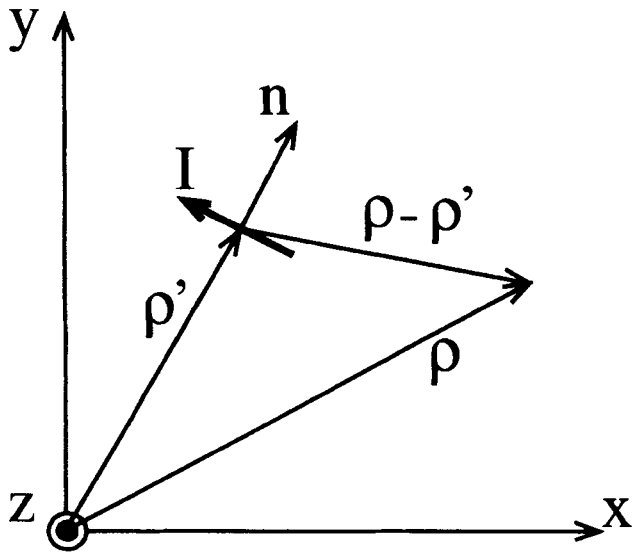

Figure 4 Element of current I

Finally, the series of emergent cylindrical modes can be obtained with the use of the discrete Fourier transform:

$$c_q = \frac{1}{2N_D H_q^{(2)}(ka)} \mathcal{F}(H_z^s)), \qquad q = -N_D, \ldots, N_D, \quad (17)$$

where $\mathcal{F}$ is defined as

$$\mathcal{F}(x) = \sum_{n=0}^{N-1} x[n] e^{-j(2\pi/N)kn}, \quad (18)$$

and H_z^s has been computed in $2N_D$ points of the cylinder of radius a that enclosed the object.

3. INTERACTION BETWEEN THE SCATTERERS

Once the individual scattering transference matrix of each object has been obtained, the iterative method described in [2] is used to analyze the scattering of all the objects. In this method, the objects are grouped progressively in sets of scatterers, and the interaction between all the sets is studied, giving place to combined transference matrices for all the objects, which take into account the presence of the rest of scatterers.

For each iteration two groups are considered, and the general formulation is summarized in the following expressions:

$$\underline{E_A} = \left(\sum_{t=1}^{M_1} \underline{T_{m2,t}} * \underline{D_t^1} \right) * \left(\sum_{t=1}^{M_2} \underline{T_{m1,t}} * \underline{D_t^2} \right) * (\underline{T_{m2,0}} * \underline{EI} + \underline{E_A}), \quad (19)$$

$$\underline{E_B} = \left(\sum_{t=1}^{M_2} \underline{T_{m1,t}} * \underline{D_t^2} \right) * \left(\sum_{t=1}^{M_1} \underline{T_{m2,t}} * \underline{D_t^1} \right) * (\underline{T_{m1,0}} * \underline{EI} + \underline{E_B}), \quad (20)$$

$$\underline{D_i} = \underline{D_i^{(1)}} * \left(\left(\sum_{t=1}^{M_2} \underline{T_{m1,t}} * \underline{D_t^2} \right) * (\underline{T_{m2,0}} * \underline{EI} + \underline{E_A}) + \underline{T_{m1,0}} * \underline{EI} + \underline{E_B} \right), \quad i = 1, 2, \ldots, M_1 \quad (21)$$

$$\underline{D_{i+M1}} = \underline{D_i^{(2)}} * \left(\left(\sum_{t=1}^{M_1} \underline{T_{m2,t}} * \underline{D_t^1} \right) * (\underline{T_{m1,0}} * \underline{EI} + \underline{E_B}) + \underline{T_{m2,0}} * \underline{EI} + \underline{E_A} \right), \quad i = 1, 2, \ldots, M_2, \quad (22)$$

where M_1 and M_2 are the number of objects of the first and second group, respectively, the subindexes $m1$ and $m2$ refer to the mean points of each group (C_{m1} and C_{m2}), the subindex 0 refers to the mean point of all first and second group objects (C_0), and $D_i^{(1),(2)}$ is the combined transference matrix for the ith object of the first (1) or second (2) group, taking into account the presence of the other objects of its own group. The $\underline{T}$ matrices are transformation matrices, as explained in [3, 4].

4. RESULTS

4.1. Computational Complexity. The computational complexity of this method can be obtained as in [5–8], but our interest consists of showing the great power of the algorithm in order to solve scattering problems that minimize the computation time.

The method has been applied to solve the scattering produced by a 4λ length metallic strip. This strip has been divided into N substrips of the same length, and N varies from 1 to 40. When N grows the needed time for finding the transference matrix of each individual strip with the use of the method of moments falls, because they are smaller strips. Only one transference matrix must be computed, because all of the strips have exactly the same length, and this matrix can be used for all of them. Moreover, when N grows the interaction algorithm is what uses the most CPU time.

However, the complexity of the method of moments is $O(n^3)$ [5] (n being the number of unknowns, which is related to the size of the scatterers), whereas the interaction algorithm has a complexity approximately linear with the number of scatterers. Then we can find a number of scatterers N that will use minimal computation time.

This process[1] is depicted in Figure 5. We can see that for $N < 10$, that is, strip lengths greater than 0.4λ, the total CPU

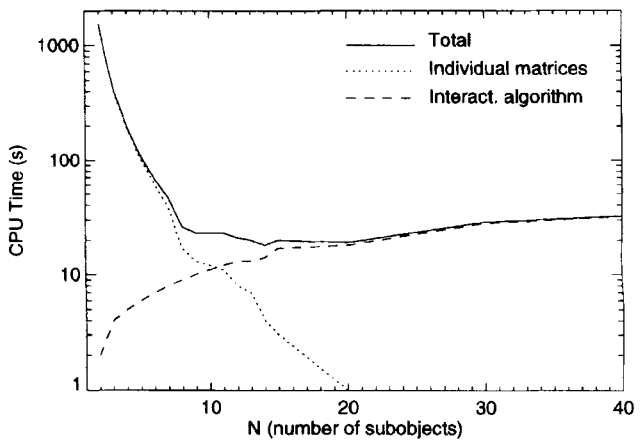

Figure 5 Comparison in terms of CPU time for a 4λ strip

[1] The simulation was performed on a PC with a 486DX4 processor, a 100-MHz clock, and 8 MB RAM, with the GNU C++ compiler.

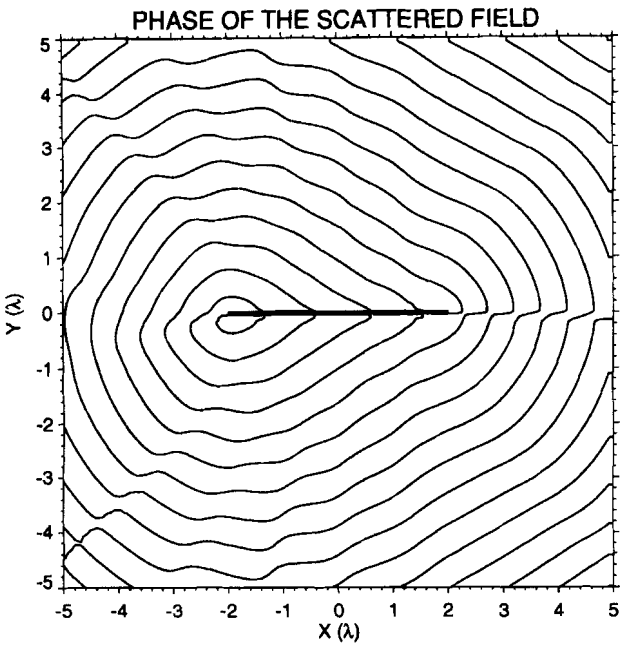

Figure 6 Phase of the scattered field by a 4λ strip obtained with 15 subelements

time is mainly dominated by the computation of the individual transference matrices with the method of moments. On the other hand, if there are more than 20 objects, the interaction algorithm becomes important in terms of the CPU time. Therefore, if we select $10 < N < 20$, the minimum is reached.

4.2. Numerical Simulations. First of all, the results for the 4λ strip used in the former section have been computed with $N = 15$. The phase of the scattered field is shown in Figure 6 when there is a plane wave incident toward $\phi = -60°$. There are two plane waves in the scattered field traveling toward $\phi = 60°$ (specular direction) and $\phi = -60°$ (shadow direction). The amplitude in the far-field region is depicted in Figure 7, and is the maximum radiation in the specular direction.

In order to assess the validity of this method a comparison with the scattered field obtained by means of the application

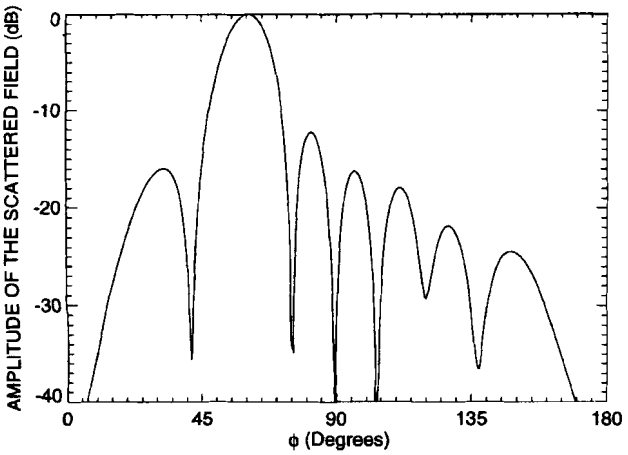

Figure 7 Amplitude of the scattered field by a 4λ strip obtained with 15 subelements

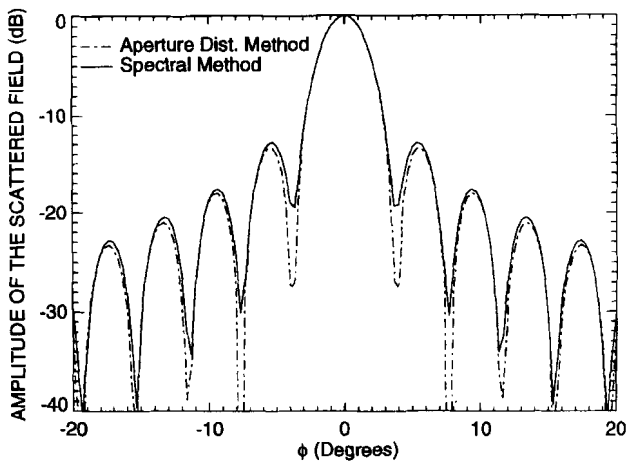

Figure 8 Comparison between this method and the aperture distribution method for the scattered field by a parabolic reflector ($f = 20\lambda$, $D = 15\lambda$) with an omnidirectional source at focus

of the aperture distribution method (with ray tracing) [9, pp. 611–617] to a parabolic reflector has been undertaken. The parabolic reflector has $f = 20\lambda$ and $D = 15\lambda$, and in our method it has been subdivided into $N = 30$ strips. Both scattered fields are shown in Figure 8. The spectral method presented in this article is more exact than the aperture distribution method, although the reflector is a sequence of strips.

Finally, because the capability of this method for large objects has been proven, an offset Cassegrain multireflector is analyzed. The offset parabolic main reflector is divided into $N = 30$ strips, and the hyperbolic subreflector into $N = 6$ strips, all with lengths of approximately $\lambda/2$. It is a clear example of great objects in terms of the wavelength. The subreflector is illuminated by a directional cylindrical source.

In Figure 9 the phase of the total field is presented. The plane wave outgoing from the parabolic reflector and an interference pattern in the area between both reflectors can

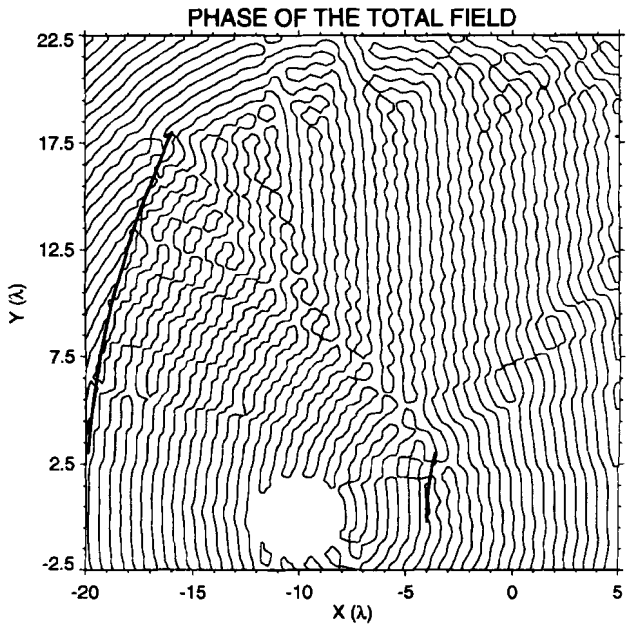

Figure 9 Phase of the total field for an offset Cassegrain multireflector

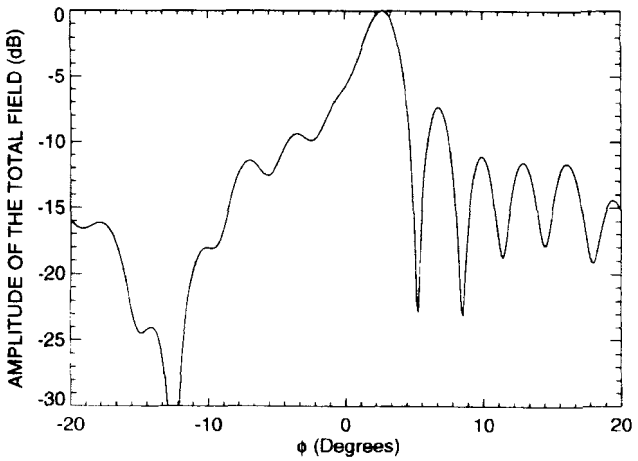

Figure 10 Amplitude of the total field for an offset Cassegrain multireflector

be observed. On the other hand, the amplitude of the total field for $-20° < \phi < 20°$ (centered in the aperture of the reflector) is shown in Figure 10. The first side-lobe level has been reduced with regard to the case of a parabolic reflector case, in spite of the offset ideal behavior, because some blockage remains. In fact, the maximum radiation is shifted a bit because of the overflow of the source field on the side of the hyperbolic subreflector. This problem has been easily studied with this method, in contrast to the ray theory usually used when analyzing reflectors problems.

5. CONCLUSIONS

A very new and efficient method for characterizing electrically large two-dimensional scatterers under TE incidence is presented. Large objects are divided into smaller ones. The complexity of this method is compared with the method of moments, and an optimum number of subdivisions for the scatterer is found in terms of the computation time.

Numerical results with the use of a strip, a parabolic reflector, and a Cassegrain multireflector system have been presented, showing the huge possibilities of this method.

REFERENCES

1. R. F. Harrington, *Field Computation by Moment Methods*, Macmillan, New York, 1968.
2. H. Esteban, V. E. Boria, M. Baquero, and M. Ferrando, "A Generalized Iterative Method for Two Dimension Scattering Problems Using Spectral Techniques," *IEE Proc. Microwaves, Antennas Propagat.*, to be published.
3. M. Baquero, "Transformaciones Espectrales y Aplicaciones a Síntesis de Ondas, Medida de Antenas y Difracción," Ph.D. thesis, Universidad Politécnica de Valencia, Valencia, 1994.
4. A. Z. Elsherbeni, M. Hamid, and G. Tian, Iterative Scattering of a Gaussian Beam by an Array of Circular Conducting and Dielectric Cylinders," *J. Electromagn. Waves Appl.*, Vol. 7, No. 10, 1993, pp. 1323–1342.
5. W. C. Chew et al., "A Generalized Recursive Algorithm for Wave-Scattering Solutions in Two Dimensions," *IEEE Trans. Microwave Theory Tech.*, Vol. MTT-40, No. 4, 1992, pp. 716–723.
6. Y. M. Wang and W. C. Chew, "An Efficient Algorithm for Solution of a Scattering Problem," *Microwave Opt. Technol. Lett.*, Vol. 3, No. 3, 1990, pp. 102–106.
7. W. C. Chew and Y. M. Wang, "A Fast Algorithm for Solution of a Scattering Problem Using a Recursive Aggregate $\bar{\tau}$ Matrix Method," *Microwave Opt. Technol. Lett.*, Vol. 3, No. 5, 1990, pp. 164–169.
8. Y. M. Wang and W. C. Chew, "Application of the Fast Algorithm to a Large Inhomogeneous Scatterer for TM Polarization," *Microwave Opt. Technol. Lett.*, Vol. 4, No. 4, 1991, pp. 155–157.
9. C. A. Balanis, *Antenna Theory. Analysis and Design*, John Wiley & Sons, New York, 1982.

Received 5-29-96

Microwave and Optical Technology Letters, 13/6, 354–358

CCC 0895-2477/96

FIELD REPRESENTATIONS IN RECIPROCAL UNIAXIAL BIANISOTROPIC MEDIA BY CYLINDRICAL VECTOR WAVE FUNCTIONS

Dajun Cheng
Wave Scattering and Remote Sensing Center
Department of Electronic Engineering
Fudan University
Shanghai 200433, People's Republic of China

KEY TERMS

Electromagnetic field, complex material, vector wave functions

ABSTRACT

Reciprocal uniaxial bianisotropic media are generalizations of the well-studied chiral materials. Based on the concept of characteristic waves and the method of angular spectral expansion, field representations in this class of media are developed in terms of the cylindrical vector wave functions. An additional theorem of vector wave functions for reciprocal bianisotropic medium can be derived from that for isotropic media. Application of the present formulations in scattering is presented to show how to use these formulations in a practical way. © *1996 John Wiley & Sons, Inc.*

I. INTRODUCTION

With recent advances in polymer synthesis techniques, increasing attention has been attracted to the analysis of interactions between electromagnetic waves and complex media. Among those novel microwave materials, reciprocal chiral media were intensively studied in the last decade. They proved to be useful to construct antireflection coatings, reciprocal microwave components, and antenna radomes. In [1], a concept of omega media with Ω-shaped metal elements embedded in a dielectric host medium was introduced to ensure the first-order effects on the propagation factor in a partially filled rectangular waveguide. These materials can find novel applications in designing reciprocal phase shifters, directional couplers, and scanning antennas [2]. A uniaxial modification of such an omega composite was proposed in [3], where the uniaxial symmetry and the additional interaction between orthogonal electric and magnetic fields make these materials potentially useful for antireflection shields and antenna radomes. Some other special cases of uniaxial materials were considered in [4–6]. Particularly, plane waves propagating in these uniaxial media were investigated. Recently, a reciprocal uniaxial bianisotropic medium was suggested to model the above-described uniaxial materials, and a vector transmis-